



BRAKING SYSTEM MODELING AND BRAKE TEMPERATURE RESPONSE TO REPEATED CYCLE

Zaini Dalimus^{a,*}

^a Electrical Engineering Department, Andalas University
Kampus Unand Limau Manis Padang, Indonesia

Received 24 April 2014; received in revised form 10 November 2014; accepted 10 November 2014
Published online 24 December 2014

Abstract

Braking safety is crucial while driving the passenger or commercial vehicles. Large amount of kinetic energy is absorbed by four brakes fitted in the vehicle. If the braking system fails to work, road accident could happen and may result in death. This research aims to model braking system together with vehicle in Matlab/Simulink software and measure actual brake temperature. First, brake characteristic and vehicle dynamic model were generated to estimate friction force and dissipated heat. Next, Arduino based prototype brake temperature monitoring was developed and tested on the road. From the experiment, it was found that brake temperature tends to increase steadily in long repeated deceleration and acceleration cycle.

Keywords: braking, kinetic energy, brake characteristic, Arduino.

1. INTRODUCTION

Driver performs braking to safely decelerate or stop the vehicle. The braking time depends on initial speed, vehicle mass, road condition and brake demand. In that short time, vehicle kinetic energy is transformed into heat energy in road-tire contact and brake contact area. At tyre slip rate of 10%, about 90% of heat energy is dissipated in friction brakes. Braking 1470 kg vehicle from 98.4 km/h to 1 km/h in 15 seconds caused the brake temperature to rise to 157°C [1].

In the development stage, friction brake is subjected to fade test. A cycle is an accelerated period of 40 seconds and followed by deceleration period of 5 seconds. After 15 cycles, it was found that the disc brake temperature reached 510°C [2]. The acceleration time is not sufficient to cool the disk through conduction, convection and radiation processes. Computer simulation known as Finite Element Method (FEM) was used to predict the temperature distribution across the disc brake and showed good results compared to lab test.

Zhang and Meng [3] used FEM model to predict disc transient temperature field and normal stress in radial with asymmetrical outer and inner disc thickness were considered. The FEM results were then validated through

experiment using thermocouples and non-contact displacement sensors. However, vehicle dynamic was not considered in calculating frictional interface pressure and total normal force.

Heat crack appears in the brake rotor surface as a result from repeated thermal stresses, compressive yield and tensile residual stress cycle [4]. Good brake rotor material has shorter average crack length for same number of stress cycles. Cho *et al.* [5] show that friction coefficient decreases noticeably when the temperature rises over 200°C, resulting in generated brake torque reduction hence increasing stopping distance. The initial brake temperature was 100°C and the test lasted for 10 minutes [5].

One way to improve brake performance is maximizing convective cooling from the rotor to surrounding airflow. Nutwell and Ramsay [6] developed CFD (Computational Fluid Dynamics) model of disc brake assembly installed on an inertia brake dynamometer. Combined with physical test, the effects of cooling air flow, braking energy input rate, and rotational speed on brake operating temperatures can be evaluated with the proposing CFD model [6]. However, the thermal load was given, not derived from real braking condition obtained from simulation or experiment.

* Corresponding Author. Phone: +62-81266224644
E-mail: zzaini21@gmail.com

II. BRAKE SYSTEM ELEMENTS

The basic braking system components in a conventional passenger car are brake pedal, linkage, master cylinder, vacuum booster, pipes, disc or drum brake assembly including slave cylinder(s), brake pads or shoes, and rotor (disc or drum). The brake pedal is a lever that amplifies the foot force F generated by the driver. Force on the pushrod F_1 is:

$$F_1 = L_P \cdot F \quad (1)$$

where L_P is brake pedal length. Since front chamber in Figure 1 is held at lower pressure P_2 either by engine inlet depression or a “vacuum” pump (e.g. on diesel engines), additional force is produced. When atmospheric air at pressure P_1 enters the rear chamber, the pressure difference generates a force F_2 on the master cylinder piston given by:

$$F_2 = (P_1 - P_2) \cdot A_1 \quad (2)$$

where A_1 is cross-sectional area of power piston and the brake booster ratio is defined as:

$$B = \frac{F_2}{F_1} \quad (3)$$

The booster ratio of modern passenger cars is typically between 4 and 9. The force on the master cylinder primary piston $F_1 + F_2$ and the generated pressure P_3 is:

$$P_3 = \frac{F_1 + F_2}{A_2} \quad (4)$$

where A_2 is cross-sectional area of brake booster. This equation does not include spring forces and seal friction forces in the master cylinder. Using the simplified cross-section of the master cylinder shown in Figure 1, the generated hydraulic actuation line pressures are:

$$P_1 = \frac{F_{mc} - F_{kl} - F_{f1}}{A_{mc}} \quad (5)$$

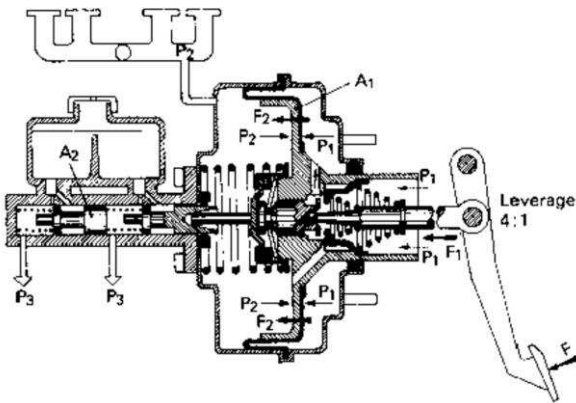


Figure 1. Pressure generation in brake system [7]

$$P_2 = P_1 - \frac{F_{k2} + F_{f2}}{A_{mc}} \quad (6)$$

where F_{mc} is master cylinder force, A_{mc} is cross-sectional of master cylinder and F_k is spring force. Therefore, the pressure in cylinder 2 is less than the pressure in cylinder 1 because of the reaction forces. Seal friction includes both static and dynamic friction and it can be estimated from:

$$F_f = \mu_s \cdot N(x) + \mu_d \cdot N \cdot \text{sign}(x) \quad (7)$$

where μ_s and μ_d are static friction and dynamic friction coefficients, x is cylinder position and N is normal force. Detailed explanation of above equations can be sourced in reference [7].

Static friction force is the force required to move the piston hydraulic seal from the stationary state, and dynamic friction occurs between the seal and the cylinder bore when the seal is sliding.

Empirical brake model is preferred since non linearity due to vacuum booster operation is taken into account. The pedal force/travel characteristic curve has three distinct regions [6]. First, the pedal moves under constant applied force from the origin to a point called “Jump-in”. Second, the pedal moves further as the applied force increases up to a point called the “Knee point”; beyond this point no additional boost force is available. These two points are shown as “A” point and “B” point in Figure 2 and are typically about 25 and 300 N. Third, the vacuum booster can’t longer amplify the applied pedal.

This third state is dangerous if reached in practice since the driver will not be able to make any significant increase in hydraulic brake line actuation pressure and thus braking force. Additionally, he/she will sense the absence of servo assistance and will interpret this as brake failure, leading to a loss of confidence and panic.

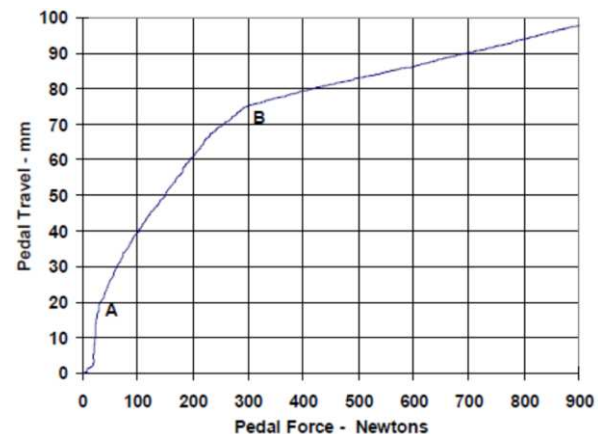


Figure 2. Pedal force/travel characteristic of a mid-size passenger car [8]

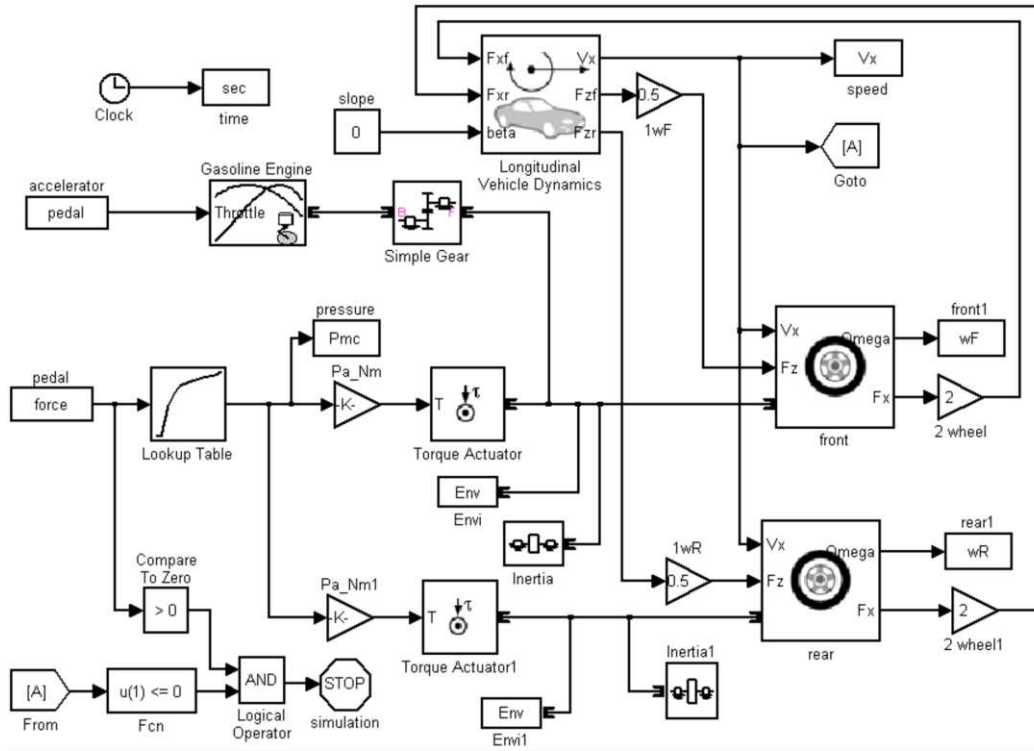


Figure 3. Two-axle vehicle model

The amount of braking torque that the friction brakes generate on one wheel is:

$$\tau_{brake} = 2 \cdot P_{line} \cdot A_c \cdot \mu_{pad} \cdot R_{disk} \quad (8)$$

for a disc brake and drum brake:

$$\tau_{brake} = P_{line} \cdot A_c \cdot (S_{leading} + S_{trail}) \cdot R_{drum} \quad (9)$$

where P_{line} is brake caliper pressure, A_c is cross-sectional of brake caliper, μ_{pad} is friction coefficient of brake pad, R_{disk} is radius of disk brake, $S_{leading}$ and S_{trail} are friction coefficient of leading and trail pads, and R_{drum} is radius of drum brake. For one axle, these torques are multiplied by 2 since the friction brake are identical. The frictional heat generated over a time period is:

$$Q_{friction} = \int \tau_{brake} \omega_{wheel} dt \quad (10)$$

where ω_{wheel} is angular speed of wheel.

III. RESEARCH METHODOLOGY

Models of basic vehicle components such as engine, tyre and chassis have been available in Matlab/Simulink software. Empirical model of brake pedal from other researchers were then programmed and combined with built-in Matlab models to produce better vehicle models. So, this research does not propose a component model but integrates all available models.

Since the heat transfer model has not been included yet, predicted brake temperature cannot be determined. Rather, road test was used to investigate temperature response of drum brake as performed in long repeated deceleration and acceleration cycle.

IV. BRAKING SIMULATION WITH MATLAB/SIMULINK

A Simulink model was then developed to predict the braking dynamics in terms of vehicle speed, wheel speeds, slip and weight transfer as shown in Figure 3; the program parameters are listed in Table 1. The tyre force is multiplied by 2 because both front tyres and rear tyres have the same braking response. The model input was either brake pedal travel or pedal force as plotted in Figure 4. In Simulink, both the pedal force and travel inputs were time-dependent series. It was

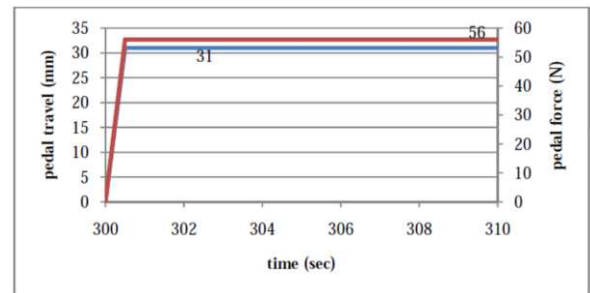


Figure 4. Driver brake input (pedal travel and pedal force)

Table 1.
Parameters

Parameters	Description	Value
m	Vehicle mass (kg)	1,500
a	Distance of front axle from the vertical projection point of vehicle CG onto the axle-ground plane (m)	1.008
b	Distance of rear axle from the vertical projection point of vehicle CG onto the axle-ground plane (m)	1.542
h	Height of vehicle CG above the ground (m)	0.569
C_d	Aerodynamic drag coefficient ($\text{Ns}^2\text{m}^{-1}\text{kg}^{-1}$)	0.346
A	Effective frontal vehicle cross-sectional area (m^2)	1.746
R_e	Effective rolling radius (m)	0.279
I_w	Wheel-tyre assembly inertia (kg.m^2)	0.5
A_{cf}	Area of front wheel cylinder (m^2)	$2 \cdot 10^{-3}$
A_{cr}	Area of rear wheel cylinder (m^2)	$0.7 \cdot 10^{-3}$
R_{disk}	Disc mean radius, $(R_o + R_i)/2$ (m)	0.105
μ_{pad}	Friction coefficient of brake pad	0.4
m_{brake}	Brake assembly mass (kg)	15
C_p	The specific heat capacity of the brake disc material	586

assumed that these inputs changed linearly with time. Both pedal travel and pedal force reached steady values of 31 mm and 56 N in 0.5 s.

Since the master cylinder pressure was modeled differently, the pressures generated were also different as shown in Figure 5. With pedal force as input, the pressure rise after 0.25 seconds. In contrast, the pressure increases as the pedal travel rise, following a quadratic function. Though the initial vehicle speeds of both models were the same at 60.4 km/h, different pressure profiles were resulted from the different braking times. The vehicle speed and its wheel translational speeds are shown in Figure 6. It was found that the braking system with pedal travel as input had a braking time of 9.9 seconds, while with the pedal force as input was 9.7 seconds. These speeds exhibit low slip since they are close each other. Compared to the front wheels, the slip of the rear wheels is smaller.

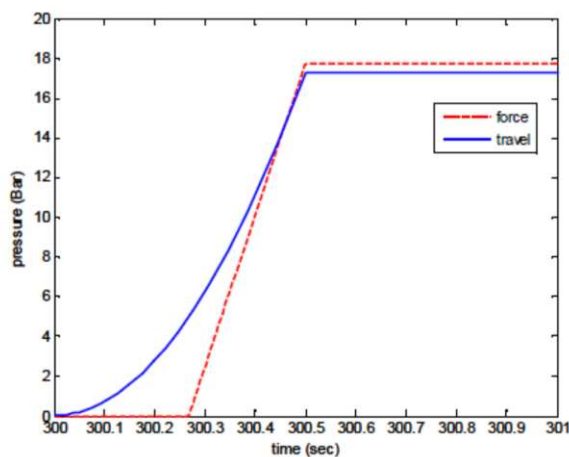


Figure 5. Hydraulic pressure generated in brake line

Brake force distribution k is defined as ratio between front braking torque to total braking torque and it can be derived from Equation (8). Assuming all the heat flows into the disc and are not conducted or convected away, the absorbed energy is:

$$Q_{\text{disk}} = m_{\text{disk}} \cdot C_p \cdot \Delta T \quad (11)$$

when 90% of kinetic energy is disposed in friction brake, energy transformation in one front wheel is given by:

$$Q_{\text{disk}} = \frac{0.9k}{2} \cdot \frac{1}{2} m_{\text{vehicle}} (V_1^2 - V_0^2) \quad (12)$$

The temperature rise prediction is found by substituting Equation (12) into Equation (11), taking into account the heat transfer mechanism by introducing factor 0.5 and there are two disk surfaces for each brake. Using vehicle data in Appendix, the front disk temperature rise was about 340°C.

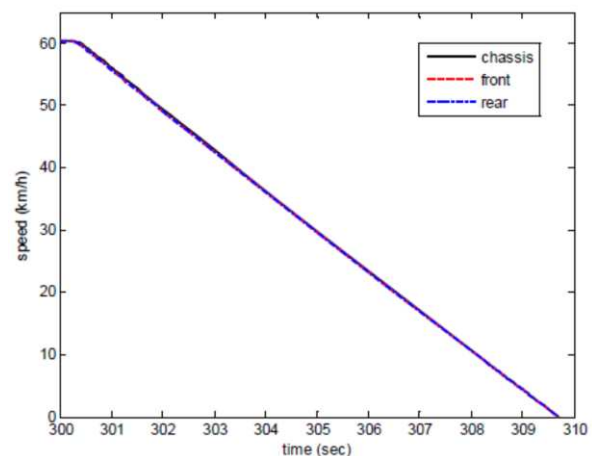


Figure 6. Vehicle road and translational wheel speeds

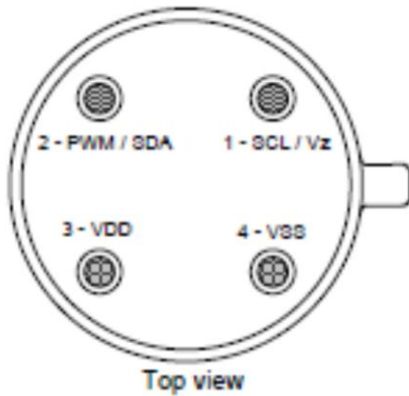


Figure 7. Pin definitions of MLX90614 thermometer [9]

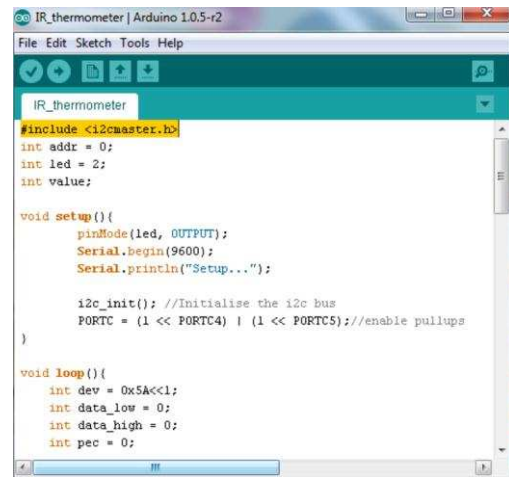


Figure 9. Arduino code for I2C communication

V. BRAKE TEMPERATURE MONITORING

A. Hardware and Software

The sensing element is contact-less infrared thermometer MLX90614 that is able to measure object temperature between -70°C up to $+380^{\circ}\text{C}$. This unit contains DSP chip performing signal conditioning and provides PWM and SMBus methods for data communication. Figure 7 shows the sensor pin definition that only needs two signals to communicate with other microprocessors. SCL/Vz is serial clock input to synchronize master and slave processors. PWM/SDA is digital input and output.

Arduino is a single-board controller designed as open-source platform that facilitates programmer to develop applications. Figure 8 shows Arduino Uno board containing Atmel AVR 16 MHz processor as the brain. There are 14 digital I/O pins and 6 analog input pins for connection with sensors and actuators. Three type memories are available in the processor chip i.e. 32 KB Flash, 2 KB SRAM and 1 KB EEPROM. To load firmware to the board, IDE Arduino 1.0.5 was used in this research.



Figure 8. Arduino Uno board

Pins connection between Arduino boards as master processor with temperature sensor unit as slave processor is shown in Table 2. To enable communication between them, a library named i2cmaster was included to Arduino program as highlighted in Figure 9. This hides low level communication from the programmer and makes reading temperature become easier. A LED was connected to digital pin 6 and would blink when temperature reading of rear brakes exceeds 150°C . This warned the driver to stop the vehicle and let the brake to cool down.

B. Result of Road Test and Analysis

During the road test, temperature sensor was fitted on the rear brake of Suzuki Carry minivan as shown in Figure 10. The sensor was positioned toward drum brake and able to measure outer surface of rear brake while driving in the Padang city. Next, Garmin GPS was used to record vehicle speed and later transferred to PC for further processing. Both vehicle speed and rear brake temperature readings were plotted on same graph to show correlation between braking event with temperature rise.

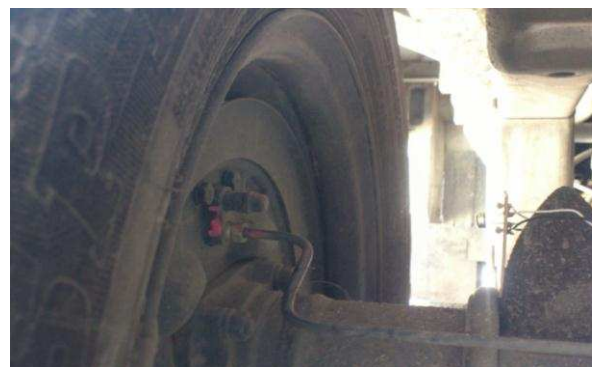


Figure 10. Sensor fitted in rear axle

Table 2.
Pins Connection between master and slave processor

Arduino	MLX90614
VCC	VDD
GND	VSS
Digital 4	SDA
Digital 5	SCL

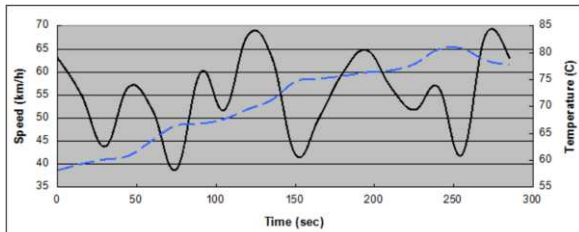


Figure 11. Vehicle speed and rear brake temperature (first test)

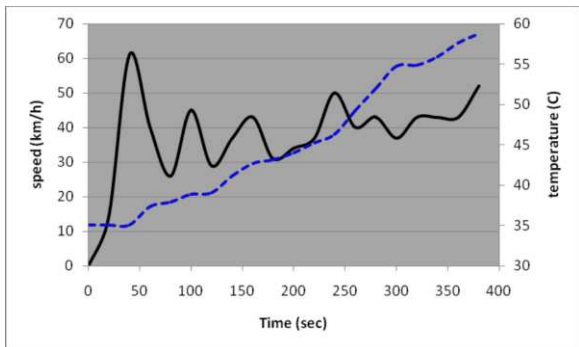


Figure 12. Vehicle speed and rear brake temperature (second test)

The solid line in Figure 11 is vehicle speed and dashed line is brake temperature profile. Repeated deceleration and acceleration cycles were performed to generate increasing brake temperature. The initial brake temperature was 58°C and vehicle speed was 63.2 km/h. After 285 seconds driving, the brake temperature became 77.8°C and thus temperature rise is 19.5°C. With brake distribution ratio between front and rear brake of 3:1, the front brake temperature was predicted to be 116.6°C calculated from $(58 + 3 \times 19.5)$.

Then, the second road test was performed as shown in Figure 12. It was confirmed that steady temperature increase was observed. After 380 seconds of driving, brake temperature rise was 23.7°C.

VI. CONCLUSION

The hydraulic pressure generated in brake line depends on brake pedal characteristic. This means same brake pedal force applied in different cars produces different brake pressures. Since the vehicle model was based on built-in Matlab/Simulink model and empirical model, the accuracy of result can be accepted. It was confirmed from the road test that repeated deceleration and acceleration cycles leads to increasing brakes temperature.

REFERENCES

- [1] L. Liang, S. Jiang and Q. Xuele, "Study on vehicle braking transient thermal field based on fast finite element method simulation," SAE Paper, No. 01-3945, 2005.
- [2] A.A. Apte and H. Ravi, "FE Prediction of thermal performance and stresses in a disc brake system," SAE Paper, No. 01-3558, 2006.
- [3] L. Zhang and D. Meng, "Theoretical modeling and FEM analysis of the thermo-mechanical dynamics of ventilated disc brakes," SAE Paper, No. 01-0075, 2010.
- [4] J.Yamabe, M. Takagi, T. Matsui, T.Kimura and M. Sasaki, "Development of disc brake rotors for trucks with high thermal fatigue strength," Japan SAE Paper, No. 4017, 2002.
- [5] M. H Choa, S. J. Kimb, D. Kimc, and H. Janga, "Effects of ingredients on tribological characteristics of a brake lining: an experimental case study," Journal of Wear, Vol. 258, 2005.
- [6] B. Nutwell and T. Ramsay, "Modeling the cooling characteristics of a disk brake on an inertia dynamometer, using combined fluid flow and thermal simulation," SAE Paper, No. 01-0861, 2009.
- [7] H. Heisler, "Advanced vehicle technology," Butterworth-Heinemann, Oxford, 2002.
- [8] J.W. Zehnder, S.S. Kanetker and C.A. Osterday, "Variable rate pedal feel emulator designs for a brake-by-wire system," SAE International, No 01-0481, 1999.
- [9] Melexis, "MLX90614 family, Single and Dual Zone Infra Red Thermometer in TO-39," Datasheet, February 2013.